Int. J. Therm. Sci. (2001) 40, 400–408

S1290-0729(01)01224-8/FLA

Parameter analysis to improve rotary desiccant dehumidification using a mathematical model

Y.J. Dai [a*], R.Z. Wang [a], H.F. Zhang [b]

[a] *Institute of Refrigeration and Cryogenics, Shanghai Jiao Tong University, Shanghai, 200030, P.R. China*

[b] *Institute of Solar Energy and Air Conditioning, Northwestern Polytechnic University, Xi'an, 710072, P.R. China*

(Received 21 February 2000, accepted 18 July 2000)

Abstract — Waves analysis using psychrometric chart, a method aiming to evaluate the rotary desiccant dehumidification, is presented in this paper. The continuity and energy conservation equations for the transient coupled heat and mass transfer are established and solved using a finite differential model. The locus of points of outlet air states along the rotational direction may be plotted as two wave fronts and one breakthrough point for both dehumidification and regeneration processes. Thermal wave, concentration wave, and middle zone point are explained in terms of the different characteristics of their own. The rules to improve the performance of dehumidification according to the wave shape are proposed and some important parameters, such as heat capacity, adsorption heat, rotation speed, regeneration temperature, thickness of the desiccant matrix and the desiccant isothermal shape, are discussed in detail using psychrometric chart. It is demonstrated that the chart method is feasible and rapid in evaluating the performance of the rotary dehumidifier. © 2001 Éditions scientifiques et médicales Elsevier SAS

desiccant dehumidification / mathematical model / thermal and concentration wave / psychrometric analysis

Nomenclature

B	atmospheric pressure	Pa
C_{pa}	specific heat of air	$J \cdot kg^{-1} \cdot K^{-1}$
C_{pl}	specific heat of water	$J \cdot kg^{-1} \cdot K^{-1}$
C_{pw}	specific heat of desiccant	$J \cdot kg^{-1} \cdot K^{-1}$
C_{pv}	specific heat of water vapor	$J \cdot kg^{-1} \cdot K^{-1}$
C_{fg}	latent heat of water	$J \cdot kg^{-1}$
C_{pz}	specific heat of supporting materials	
D_{eff}	effective diffusivity of desiccant	$m^2 \cdot s^{-1}$
f_V	ratio of desiccant surface area to volume	$m^2 \cdot m^{-3}$
f_S	ratio of free flow area to section area of rotary wheel	
K_Y	coefficient of mass convection	$kg \cdot m^{-2} \cdot s^{-1}$
L	thickness of the desiccant matrix	m
m_i	mass flow of air per unit section area of rotary wheel	$kg \cdot m^{-2} \cdot s^{-1}$
M_w	desiccant mass per unit volume	$kg \cdot m^{-3}$
M_z	mass of supportive structure per unit volume	$kg \cdot m^{-3}$
P_s	saturation pressure	Pa
Q	adsorption heat	$J \cdot kg^{-1}_{water}$
r_1	radius of the matrix axis	m
r_2	radius of the rotary wheel	m
RH	relative humidity	
t	temperature of air	°C
T	temperature	K
t_w	temperature of desiccant	°C
T_{db}	dry bulb temperature of the air	°C
V_d	velocity of dehumidification air stream	$m \cdot s^{-1}$
V_r	velocity of regeneration air stream	$m \cdot s^{-1}$
W	water content of desiccant	$kg_{water} \cdot kg^{-1}_{adsorbent}$
Y	humidity ratio	$kg_{moisture} \cdot kg^{-1}_{dry\ air}$
Y_w	humidity ratio near the wall of desiccant	$kg_{moisture} \cdot kg^{-1}_{dry\ air}$

Greek symbols

α	coefficient of heat transfer	$W \cdot m^{-2} \cdot K^{-1}$
ρ	density	$kg \cdot m^{-3}$
λ	thermal conductivity of desiccant	$W \cdot m^{-1} \cdot K^{-1}$

* Correspondence and reprints.
E-mail address: yjdai@sh163.net (Y.J. Dai).

τ	time	s
ω	rotation speed	s^{-1}
r, φ, Z	polar coordinates	
φ_R	angle of regeneration section	

1. INTRODUCTION

Desiccant dehumidification is advantageous in dealing with latent load and improving indoor air quality (IAQ), because desiccant adsorbs moisture directly and captures the contamination of the air simultaneously. Desiccant dehumidifier, running in open cycle and also characterized by no noise and convenience in maintenance, can be driven by low grade heat sources, e.g., solar energy, waste heat and natural gas.

To assess the performance of rotary desiccant dehumidifier for given operating conditions, lots of work on simulation has to be carried out. Such work requires methods that allow rapid and accurate evaluation of the investigating results. Many mathematical models on the rotary desiccant dehumidifier have been proposed in the past decades. Maclaine-Cross developed MOSHMX, a finite difference computer program based on a detailed numerical analysis [1]. DESSIM was written by Barlow where the dehumidifier was discretized and each node was treated as a counter flow heat and mass exchanger in which both the heat and mass transfer are assumed to be uncoupled [2]. Collier and Cohen developed ET/DESSIM, which is more accurate by means of incorporating several improvements over the DESSIM program [3]. The research group of Worek also developed a mathematical model and made success in predicting the performance and optimizing the operation parameters of rotary desiccant wheels [4–6].

Macline-Cross and Banks developed two functions, F_1 and F_2, correlating psychrometric states with two independent characteristic parameters [7]. Van den Bulck et al. proposed a designing wave analysis method that includes the effects of "shocks" based on F_1 and F_2 chart [8, 9].

In China, Yu et al. have made efforts to complete a new mathematical model concerning the complicated heat and mass transfer in the rotary desiccant matrix [10]. These models are helpful for predicting the performance and evaluating the benefits of rotary desiccant wheel but are not brief enough. Key problem is how to organize the numerical results efficiently and give a definite conclusion rapidly. Here a systematic analysis method is completed, aiming to evaluate the system performance effectively, and to optimize the rotary desiccant dehumidifier.

The objective of this paper is to present the wave analysis method using psychrometric chart and analyze the effects of some parameters with a mathematical model in order to improve the rotary desiccant dehumidification.

2. WAVES ANALYSIS USING PSYCHROMETRIC CHART

If the air states at the outlet of the desiccant wheel are plotted in the psychrometric chart, two wave shape curves are obtained, the upper one is the record for regeneration section and the lower is that for dehumidification. A constant elapsed time exists between each point plotted. In the dehumidification range, three parts can be classified, namely, thermal wave, concentration wave and middle zone condition or the MZ point that exists between the two passing wavefronts. The thermal wave, spreading from regeneration condition to a point of minimum absolute humidity, is characterized by short time period and is strongly dependent on the total heat capacity. Corresponding to this process, the adsorbent with high temperature rotates out of the regeneration section, the equilibrium water vapor pressure at the desiccant surface is high, and the adsorbent hence cannot adsorb water vapor effectively. The temperature of the adsorbent experiences a stronger variation than water content does. The position has been called the middle zone condition or the MZ point. The outlet air remains at or near this condition for some time, and then experiences the gradual breakthrough of the main concentration wave, which forms the locus of points that connects this minimum absolute humidity point with the inlet air conditions. The concentration wave may last a long time period, and is determined mainly by thermal effects of adsorption. A condition identical to that of the dehumidification process also exists for the regeneration process. The first and fastest wavefront describes the locus of points that begin at the dehumidifier inlet conditions and progresses quickly to a point of maximum outlet humidity. The air remains at this condition for a period of time and then experiences breakthrough of the main concentration front, with the outlet conditions gradually approaching the inlet regeneration air conditions. The variations of water content for adsorbent, both in dehumidification and regeneration, occur mostly in this zone rather than in thermal wave controlled area.

Psychrometric chart corresponding to the above two wavefronts is shown in *figure 1*. The separated points stand for outlet states of the air for both dehumidifi-

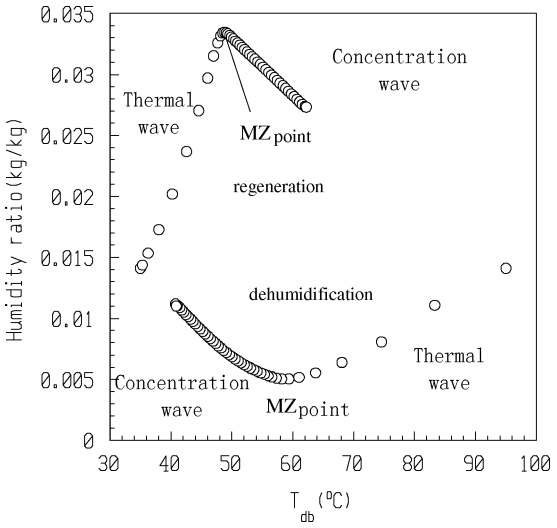

Figure 1. Psychrometric waves chart.

cation and regeneration processes. The system performance is dominated by the average outlet air conditions that represent the time- or position-averaged effects of both the first and second waves associated with the heat and mass transfer within the desiccant matrix. The lower the absolute humidity, the higher the dehumidification capacity of the system will be. The higher the temperature, the higher the preheating temperature of the regeneration air. This reduces the amount of external thermal energy and thereby increases the thermal COP. On the dehumidification side, moist air corresponding to the thermal wave is in humid and hot condition. The mean outlet temperature and humidity increase with the decrease of the speed of thermal wave of MZ point and inlet regeneration air state. The most advantageous thermodynamic conditions for optimal cycle operation are the two MZ points associated with both the dehumidification and regeneration processes. Rules to optimize the performance of the dehumidifier are:

- The faster the speed of the thermal wave and the steeper the slop of the thermal wave, the better the performance of the dehumidifier will be.
- The concentration wave should be slow and smooth and its locus should be kept as close to the MZ point (the thermal dynamic optimum) as possible.
- MZ point should be low and close to the right side in the psychrometric chart for dehumidification, and high and close to the left side for regeneration.

3. MATHEMATICAL MODEL AND PSYCHROMETRIC CHART

3.1. Mathematical model

Four equations concerning water content balance and energy conservation are used to describe the complicated heat and mass transfer occurring in moisture adsorption and regeneration. Assumptions to obtain equations (1)–(4) are given below:

- Effect of centrifugal force is neglected due to low rotation speed of the rotary dehumidifier.
- No leakage takes place between dehumidification and regeneration sections.
- Shell of the rotary dehumidifier satisfies the insulated condition.
- No pressure loss along Z direction.
- Heat and mass transfer in radius direction is not taken into consideration.
- Desiccant is uniformly distributed in the matrix, f_V, f_S are constant.
- Isotropic thermal conductivity and diffusivity.

Conservation of moisture for the processed air:

$$\frac{\partial Y}{\partial \tau} + \omega \frac{\partial Y}{\partial \varphi} + \frac{m_i}{\rho_i f_S} \frac{\partial Y}{\partial Z} = \frac{K_Y f_V}{\rho_i f_S}(Y_w - Y) \quad (1)$$

Conservation of energy for the process air:

$$\frac{\partial t}{\partial \tau} + \omega \frac{\partial t}{\partial \varphi} + \frac{m_i}{\rho_i f_S} \frac{\partial t}{\partial Z} = \frac{\alpha f_V}{\rho_i f_S (C_{pa} + Y C_{pv})}(t_w - t) \quad (2)$$

Conservation of water content for the absorbent:

$$\frac{\partial W}{\partial \tau} + \omega \frac{\partial W}{\partial \varphi} - D_{eff}(1 - f_S)\left[\frac{2\ln(r_2/r_1)}{r_2^2 - r_1^2}\frac{\partial^2 W}{\partial \varphi^2} + \frac{\partial^2 W}{\partial Z^2}\right] = \frac{K_Y f_V}{M_w}(Y - Y_w) \quad (3)$$

Conservation of energy for the absorbent:

$$\frac{\partial t_w}{\partial \tau} + \omega \frac{\partial t_w}{\partial \varphi} - \frac{\lambda(1 - f_S)}{M_w(C_{pw} + W C_{pl}) + M_z C_{pz}} \cdot \left[\frac{2\ln(r_2/r_1)}{r_2^2 - r_1^2}\frac{\partial^2 t_w}{\partial \varphi^2} + \frac{\partial^2 t_w}{\partial Z^2}\right] = \frac{1}{M_w(C_{pw} + W C_{pl}) + M_Z C_{pz}} \cdot \left[\alpha f_V (t - t_w) + K_Y f_V (Y - Y_w) Q\right] \quad (4)$$

where Q stands for heat of adsorption.

In the above four equations, the air humidity ratio near the wall of absorbent is unknown, therefore, three auxiliary relations are needed:

$$Y_{\mathrm{w}} = \frac{0.622\,RH \cdot P_{\mathrm{S}}}{B - RH \cdot P_{\mathrm{S}}} \tag{5}$$

$$\ln P_{\mathrm{S}} = 23.1964 - \frac{3\,816.44}{t_{\mathrm{w}} - 46.13} \tag{6}$$

$$\frac{W}{W_{\max}} = \frac{RH}{R + (1-R)\,RH} \tag{7}$$

Here, B is the atmospheric pressure, P_{S} stands for the saturation pressure of moisture at the wall temperature of adsorbent. $W/W_{\max}$ is relative adsorption rate, $W_{\max}$ stands for the maximum adsorption rate of absorbent. R, an important parameter which reflects the desiccant isotherm shape, is called separation factor of adsorbent. RH is the relative humidity of air. Seven unknowns are involved in seven equations, so they all have definite solutions.

Boundary conditions are:

- For regeneration section, if $2\pi - \varphi_{\mathrm{R}} \le \varphi < 2\pi$, then $Y_{\mathrm{in}} = Y_2$, $t_{\mathrm{in}} = t_2$.
- For dehumidification section, $0 \le \varphi < 2\pi - \varphi_{\mathrm{R}}$, then $Y_{\mathrm{in}} = Y_1$, $t_{\mathrm{in}} = t_1$.

In addition, the periodic boundary conditions are given as

$$Y(0, Z, \tau) = Y(2\pi, Z, \tau), \qquad t(0, Z, \tau) = t(2\pi, Z, \tau)$$
$$W(0, Z, \tau) = W(2\pi, Z, \tau), \quad t_{\mathrm{w}}(0, Z, \tau) = t_{\mathrm{w}}(2\pi, Z, \tau)$$

If the transient problem is taken into consideration, the initial conditions are also necessary:

- For desiccant, $W(\varphi, Z, 0) = W_0$, $t_{\mathrm{w}}(\varphi, Z, 0) = t_0$.
- For dehumidification air stream, $0 \le \varphi < 2\pi - \varphi_{\mathrm{R}}$, $Y(\varphi, Z, 0) = Y_1$, $t(\varphi, Z, 0) = t_1$.
- For regeneration air stream, $2\pi - \varphi_{\mathrm{R}} \le \varphi < 2\pi$, $Y(\varphi, Z, 0) = Y_2$, $t(\varphi, Z, 0) = t_2$.

Here, t_1 and t_2 denote the inlet air temperatures for dehumidification section and regeneration section, respectively, t_0 and Y_0 stand for temperature and humidity ratio at initial conditions, and Y_1, Y_2 stand for inlet air humidity for dehumidification and regeneration sections.

The reason that this model is preferable lies in that it accounts for the effect of mass diffusion and heat diffusion, the precision of governing equations to describe the physics of rotary dehumidifier is thus enhanced.

3.2. Numerical resolution

Equations (1)–(4), in which time and space variation terms are included, can be discretized into finite difference equation group. For space varying terms, two kinds of difference schemes, one order upwind difference scheme for the convection terms and central difference scheme for the diffusion terms, are adopted. For time variation terms, different schemes are used according to the variation of ε, they are fully implicit, semi-implicit (Crank–Nicholson) and explicit schemes relative to $\varepsilon = 1, 0.5, 0$, respectively. Difference scheme should satisfy the demands of computation. To compute steady state, fully implicit scheme is recommended because of its reliability of convergence. To investigate the dynamic behavior of dehumidification device, explicit scheme, typical time step method which does not need the iteration process, is usually employed. Owing to the constraints of stability, time step should be small enough, or the divergence of solution cannot be avoided. In addition, small time step is also numerically necessary for accurate computation. Iterative computation have to be carried out at a fixed time period for semi-implicit scheme, a proper mesh size should be specified to save computation time.

3.3. Wave chart plotting

The psychrometric wave chart can be obtained by numerical and experimental investigations on condition that the outlet air states at different points of both dehumidification and regeneration sides are known.

In this study, the chart was attained by numerical method using the computation program developed from the above model. To check the accuracy of the mathematical model, regular density (RD) silica gel is chosen as desiccant and several auxiliary equations are appended meanwhile. The calculation conditions of the base case are listed in *table I*. Coefficients of heat and mass transfer are given below [11]:

- Coefficient of mass transfer:

$$K_Y = 0.704 \dot{m}_i\, Re^{-0.51}\ [\mathrm{kg{\cdot}m^{-2}{\cdot}s^{-1}}] \tag{8}$$

- Coefficient of heat transfer:

$$\alpha = 0.671 \dot{m}_i\, Re^{-0.51} C_{\rho \mathrm{e}}\ [\mathrm{W{\cdot}m^{-2}{\cdot}K^{-1}}] \tag{9}$$

TABLE I
Calculation conditions of the base case.

Parameter	Value	Parameter	Value	Parameter	Value
Thickness L	0.2 m	C_{pw}	921.0 kJ·kg^{-1}·K^{-1}	T_{in}	35 °C
r_1	0.05 m	C_{pz}	921.0 kJ·kg^{-1}·K^{-1}	RH_{in}	40 %
r_2	0.25 m	λ	0.14417 W·m^{-1}·K^{-1}	W_{max}	0.4 kg·kg^{-1}
f_S	0.194 m^2·m^{-2}	D	2.4·10^{-6} m^2·s^{-1}	ω	5 r·h^{-1}
f_V	1 468.85 m^2·m^{-3}	V_d	2.86 m·s^{-1}	Q	equation (8)
M_w	720.06 kg·m^{-3}	V_r	2.86 m·s^{-1}		
M_z	720.06 kg·m^{-3}	φ_R	180°		

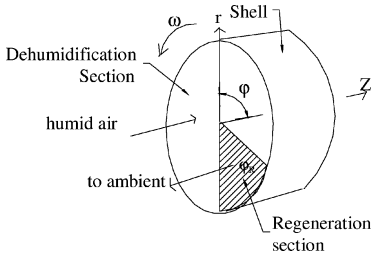

Figure 2. Coordination diagram of desiccant matrix.

The adsorption heat of regular density silica gel in kJ·kg$^{-1}_{water}$ is calculated by Pesaran and Mills [12]:

$$Q = \begin{cases} -13\,400W + 3500, & W \le 0.05 \\ -1\,400W + 2\,950, & W > 0.05 \end{cases} \quad (10)$$

The equilibrium isotherm is given as

$$RH = 0.0078 - 0.05759W + 24.16554W^2 - 124.78W^3 + 204.226W^4 \quad (11)$$

The practical isotherm of the specified desiccant may be analogous to the isotherm type characterized by a fixed R in equation (7).

Looking at the three diffusion mechanisms for adsorption of RD silica gel, namely, ordinary diffusion, Knuson diffusion and surface diffusion, Pesaran thought that the surface diffusion is dominant [12]. The surface diffusivity is given as

$$D_S = D_0 \exp\left[-0.974\cdot10^{-3}\frac{Q}{T+273.15}\right] [\mathrm{m^2\cdot s^{-1}}] \quad (12)$$

D_0 is 0.8·10^{-6} m^2·s^{-1}. Q is the heat of adsorption (in J·kg^{-1}).

The transient numerical results are in good agreement with those from Collier et al. [13]. *Figures 3* and *4* show the cases with regeneration temperature of 95 °C and 120 °C, respectively.

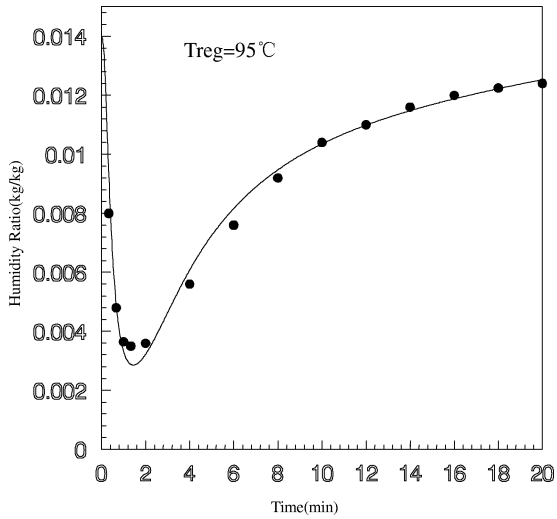

Figure 3. Dynamic behavior of RD silica gel at regeneration temperature. $T = 95$ °C. Points, data from Collier et al. [13]; line, simulated result.

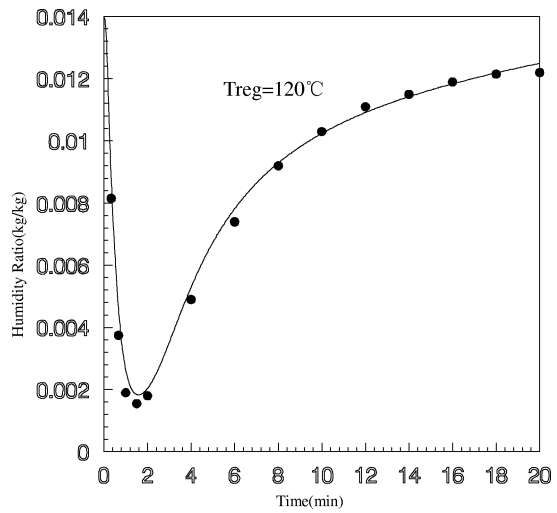

Figure 4. Dynamic behavior of RD silica gel at regeneration temperature. $T = 120$ °C. Points, data from Collier et al. [13]; line, simulated result.

4. ANALYSIS

Using the waves analysis in psychrometric chart incorporating with numerical calculation, several parameters, which have strong influence on the system performance, are discussed. For each case, only the value of the discussed parameter varies while the other parameters are kept constant.

4.1. Heat capacity

Figure 5 shows the effect of heat capacity clearly under a given regeneration temperature. With the increase of the heat capacity, the MZ point moves up for dehumidification but down towards left corner for regeneration in the chart. In addition, thermal wave becomes slow and occupies more time fraction during the whole rotation period. The concentration wave becomes sharp and the slope is steeper. As a result, the average outlet humidity and temperature rise in dehumidification and fall in regeneration. This is beneficial to increase the preheating temperature for the regeneration air in desiccant cooling system and thus increase the system COP, but is unbeneficial just from the point of view of dehumidification. It is, therefore, reasonable to seek a balance between adding inert heat capacity material and choosing desiccant materials.

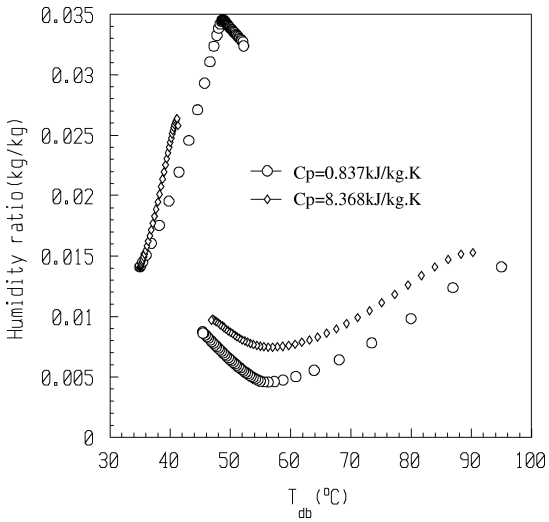

Figure 5. Impact of heat capacity.

4.2. Adsorption heat

Here, two kinds of adsorption heat characteristic relations instead of equation (10) are analyzed, namely, constant adsorption heat and linear relationship that adsorption heat decreases with the increase of adsorption rate. It is obvious (*figure 6*) that the performance reflected by the first curve (constant adsorption heat) is poor and that of the second is better. Generally, the second relation is more approximate to the practice. It is shown in *figure 6* that for regeneration the slope of concentration wave becomes steeper and the MZ point climbs higher as the adsorption heat decreases with the increase of the adsorption rate. For dehumidification, the range of variation for concentration wave becomes wider, the slope becomes smooth and the MZ point also climbs higher if the adsorption heat keeps constant.

Generally speaking, it is expected that the adsorption heat drops with the increase of adsorption rate significantly. Thus, the ideal wave shape is maintained so that the reliability and the economic feasibility of the dehumidifier can be ensured. From the viewpoint of regeneration the heat to regenerate the desiccant can be used efficiently because most of the heat is utilized in driving water from the desiccant.

4.3. Maximum water content

The maximum water content is one of the most important characteristics for desiccant materials.

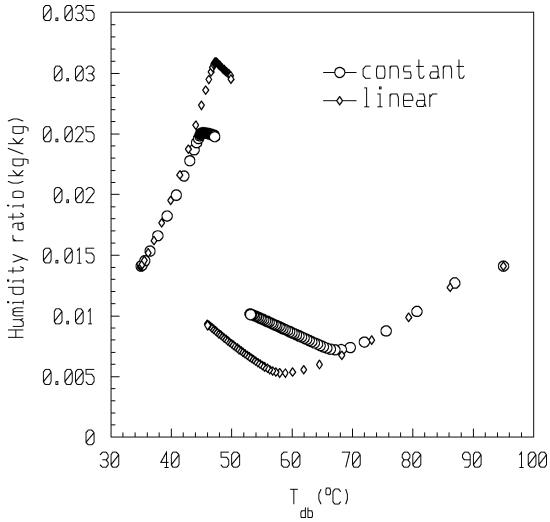

Figure 6. Impact of adsorption heat.

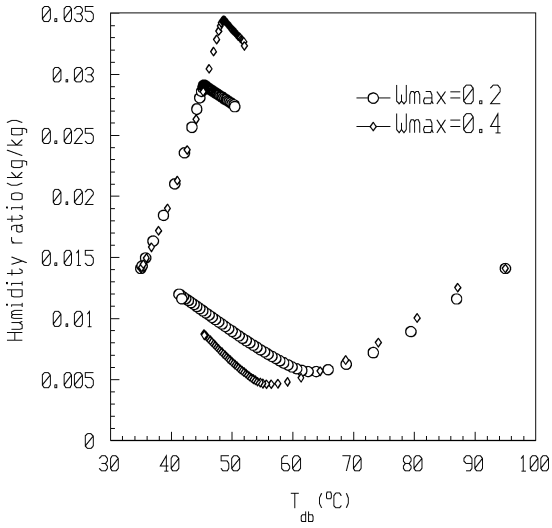

Figure 7. Impact of the maximum water content.

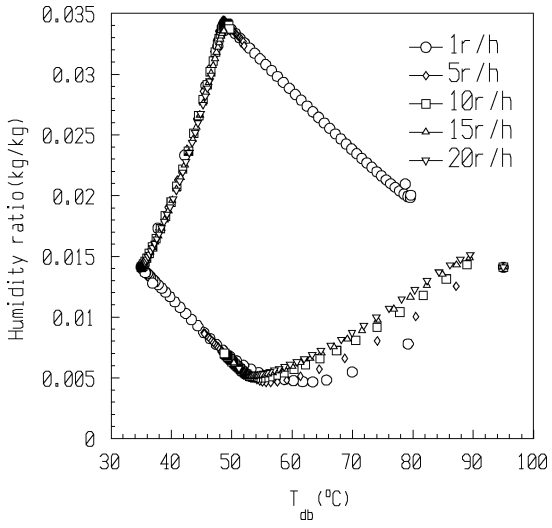

Figure 8. Impact of rotation speed.

As shown in *figure 7*, when W_{max} varied from 0.2 to 0.4 $kg_{water} \cdot kg_{desiccant}^{-1}$, the thermal wave becomes slow and occupies a longer time period fraction but changes slightly in slope, the concentration wave hence varies in a smaller range and becomes steep. The MZ point moves down on the left for dehumidification and up on the right for regeneration, which means that the overall performance of the dehumidifier is improved.

4.4. Rotation speed

The effect of rotation speed on the wave shape is concluded as follows (*figure 8*):

- No effect on MZ point.
- Larger fraction of the time period for thermal wave with increasing of rotation speed.
- Little change of the slopes of both thermal and concentration waves.

Figure 8 shows the wave shape variation caused by changing rotation speed. There should be an optimum rotation speed from the viewpoint of psychrometric waves analysis. With regard to the optimum rotation speed, the thermal wave becomes fast and the concentration wave concentrates to a small range in the psychrometric chart. Thus, good performance both for dehumidification and regeneration processes can be ensured. The other important aspect for increasing the rotation speed of the desiccant wheel is represented by increased adsorption rate and decreased adsorption heat, also resulting to higher outlet average temperature, lower average humidity in the dehumidification section, and lower average outlet temperature, higher outlet average humidity in regeneration section.

4.5. Regeneration temperature

As shown in *figure 9*, the rising of regeneration temperature contributes mainly to the variation of the MZ point, reflected by moving up on the right side for regeneration and down on the right side for dehumidification. In the regeneration range there is little response on the

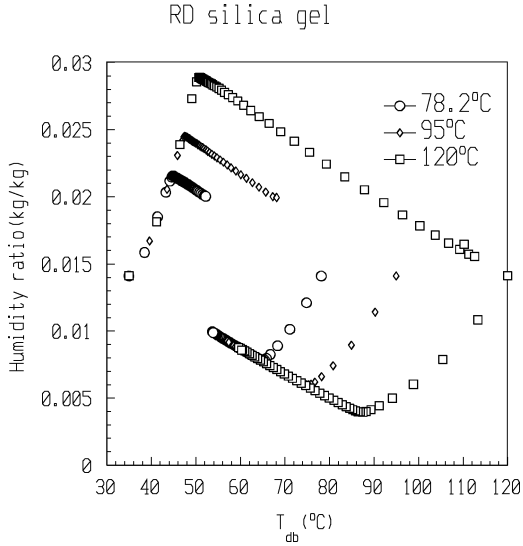

Figure 9. Impact of regeneration temperature.

thermal wave to the change of regeneration temperature, but the concentration wave shows strong dependence. The higher the regeneration temperature, the larger range the concentration wave will cover. It seems to be no effect on the slope of concentration wave. Usually, higher regeneration temperature is necessary for deep dehumidification, while much more heat has to be added to the regeneration air which is unbeneficial to increase COP. A balanced regeneration temperature should be specified regarding COP and the dehumidification practice.

4.6. Thickness of the desiccant matrix

Thick desiccant matrix makes the thermal wave spread faster, the concentration wave at dehumidification becomes steeper and the locus of the concentration wave points are concentrated more densely, as *figure 10* shows. The MZ point moves down a little bit, while the outlet average temperature becomes higher and the humidity becomes lower. For regeneration, the MZ point moves up a little bit, the outlet temperature drops imperceptible and the humidity rises at the same time. The performance of dehumidifier can be improved by increasing the thickness of the adsorption bed below the maximum allowable thickness. In practice, the maximum allowable thickness of the desiccant matrix is determined by pressure losses. *Figure 10* shows that under the conditions given in this paper, the wave fronts change significantly when the bed thickness increases from 10 to 20 cm, while only slight change occur if the thickness is above 20 cm.

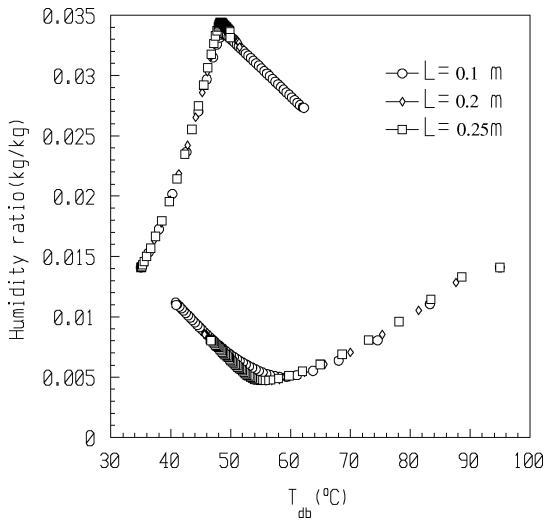

Figure 10. Impact of matrix thickness.

4.7. Isotherm shape

To assess the effect of isotherm shape, equation (7) is used instead of equilibrium equation (11) of RD silica gel, but the other parameters are set in accordance with *table I*.

The desiccant isotherm shape is the most important factor in determining the wave front shapes within the desiccant matrix. This isotherm is described by equation (7). Under two cases, setting the regeneration temperatures at 78.2 and 120 °C, respectively, effects of the separation factor of isotherm shape are discussed in the following, which are shown in *figures 11* and *12*. Here R varies from 0.01 to 1.0.

In the case of regeneration at 78.2 °C, in regeneration the MZ point moves down with decreasing R. Within the range of R from 0.05 to 0.1 the MZ point reaches its highest position, thereafter the MZ point begins to drop and assumes its lowest point at $R = 1.0$. The influence of isotherm shape on the thermal wave is concluded as following, the smaller the value of R the steeper the slope of the thermal wave front and the larger range of concentration wave will be. The smaller the value of R, the higher the MZ point and the faster the thermal wave will be. For dehumidification, there exists a turnover point approximately at $R = 0.1$ or 0.05 (slight difference between them). Whether R increases or decreases apart from that value, the MZ point will always move up. The higher the MZ point, the faster the thermal wave will become. The concentration wave is most densely

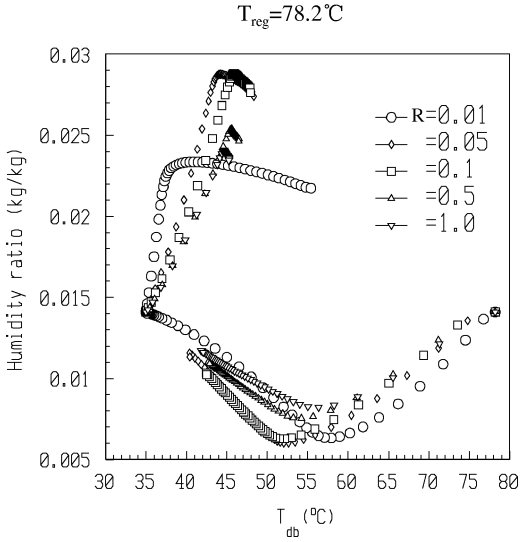

Figure 11. Impact of isotherm shape at low regeneration temperature.

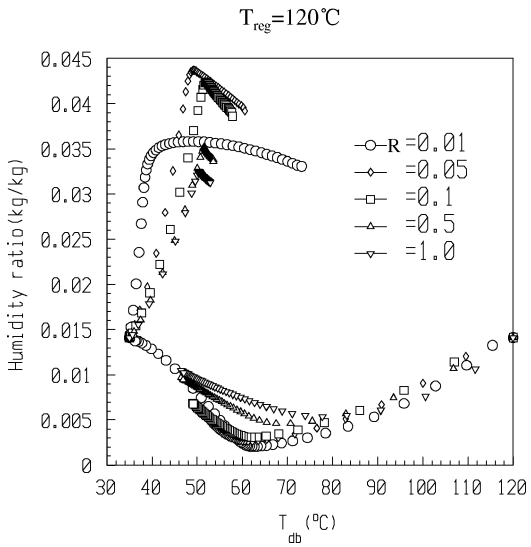

Figure 12. Impact of isotherm shape at high regeneration temperature.

distributed at $R = 0.1$ or 0.5, second densely at $R = 0.05$ or 1.0 and poorest at $R = 0.01$. The compromise isotherm shape, therefore, should be $R = 0.1$, it is called type 1M [14].

In the case of regeneration at 120 °C the similar analysis is conducted. It is found that the isotherm shape should be $R = 0.05$.

Comparing the two cases with low and high regeneration temperature, we can conclude that the compromise isotherm shape parameter to obtain the optimum performance decreases with the increase of the regeneration temperature.

5. CONCLUSIONS

The mathematical model presented in this paper is capable to predict the performance of rotary desiccant wheel. The numerical results are in good agreement with those from [13]. The psychrometric waves chart analysis, in combination with finite difference model or other methods, enables rapid evaluation of the performance of desiccant wheel and is of assistance to designing and manufacturing. Only according to the criteria of ideal wave shapes the merits and drawbacks of a given set of operation parameters can be concluded properly.

REFERENCES

[1] Maclaine-Cross I.L., Proposal for a desiccant air conditioning system, ASHRAE Trans. 94 (2) (1988) 1997–2009.

[2] Davanagere B.S., Sherif S.A., Goswami D.Y., A feasibility study of a solar desiccant air-conditioning system, Part I: Psychrometrics and analysis of the conditioned zone, Int. J. Energy Res. 23 (1999) 7–21.

[3] Collier R.K., Cohen B.M., An analytical investigation of methods for improving the performance of desiccant cooling system, ASME J. Solar Energy Engrg. 113 (1991) 157–163.

[4] Charoensupaya D., Worek W.M., Parametric study of an open-cycle adiabatic, solid, desiccant cooling system, Energy 13 (1988) 739–749.

[5] Zheng W., Worek W.M., Novesel D., Performance optimization of rotary dehumidifiers, ASME J. Solar Energy Engrg. 117 (1995) 40–44.

[6] Zheng W., Worek W.M., Novosel D., Effect of operating conditions on optimal performance of rotary dehumidifiers, ASME J. Solar Energy Engrg. 117 (1995) 62–66.

[7] Maclaine-Cross I.L., Banks D.J., Coupled heat and mass transfer in regenerators — prediction using an analogy with heat transfer, Int. J. Heat Mass Tran. 15 (1972) 1225–1242.

[8] Van den Bulk E., Mitchell J.W., Klein S.A., Design theory for rotary heat and mass exchangers, I. Wave analysis of rotary heat and mass exchangers with infinite transfer coefficients, Int. J. Heat Mass Tran. 28 (1985) 1575–1586.

[9] Van den Bulk E., Mitchell J.W., Klein S.A., Design theory for rotary heat and mass exchangers, II. Effectiveness-number-of-transfer-units method for rotary heat and mass exchangers, Int. J. Heat Mass Tran. 28 (1985) 1587–1595.

[10] Yu J.D., Luo G., Zhang H.F., New mathematical model of a rotary desiccant wheel and the program of RDCS. Tai Yang Neng Xuebao, Acta Energiae Solaris Sinica 16 (1995) 366–378 (in Chinese).

[11] Pla-Barby F.E., Vliet G.C., Rotary bed solid desiccant drying: An analytical and experimental investigation, in: Joint ASME/AICHE 18th National Heat Transfer Conference, San Diego, CA, August 6–8, 1979, pp. 7–8.

[12] Pesaran A.A., Mills A.F., Moisture transport in Silica Gel packed beds, II. Experimental study, ASHRAE, 1992.

[13] Collier R.K., Cohen B.M., Slosberg R.B., Desiccant properties and their effects on the performance of desiccant cooling systems, ASHRAE, 1992, pp. 75–81.

[14] Collier R.K., Cale T.C., Lavan Z., Advanced desiccant materials assessment, GRI-8610181, Gas Research Institute, Chicago, III, 1986.

[15] Jurinak J.J., Mitchell J.W., Beckman W.A., Open cycle desiccant air conditioning as an alternative to vapor compression cooling in residential applications, ASME J. Solar Energy Engrg. 106 (3) (1985) 252–260.